An Opening Displacement Curve Characteristic Determined by High-Current Anode Phenomena of a Vacuum Interrupter

Liqiong Sun, Li Yu, Zhiyuan Liu, *Member, IEEE*, Jianhua Wang, and Yingsan Geng, *Member, IEEE*

***Abstract*—A vacuum interrupter reaches its interruption limit once high-current anode phenomena occur. In order to increase the interrupting capability of vacuum interrupters, extensive research work has been done which included consideration on the contact geometry, contact material, and magnetic field in order to avoid the formation of high-current anode phenomena. However, an opening displacement curve characteristic of a movable contact should be another contributor to the formation of high-current anode phenomena. The objective of this paper is to propose an opening displacement characteristic that is determined by high-current anode phenomena of a vacuum interrupter. Butt-type contacts were used in the test vacuum interrupters and the contact diameters were 12 mm and 25 mm, respectively. The contact materials were microcrystalline CuCr25 and nanocrystalline CuCr25, respectively. Two different opening velocities were tested which were 1.1 m/s and 2.0 m/s, respectively. In the tests, the arcing time was adjusted from ∼1 ms to 10 ms at each velocity. Test results showed that each type of vacuum interrupter has its own anode discharge diagram which is irrespective of the opening velocities. Based on each anode discharge diagram, an opening displacement curve can be proposed in order to avoid the regions of an intense arc mode and an anode spot mode. With the proposed opening displacement curve, high-current anode phenomena have less of an impact on the arcing period, which is expected to improve the interrupting performance of the vacuum interrupter.**

***Index Terms*—Anode discharge diagram, anode phenomena, vacuum arc, vacuum interrupter.**

I. Introduction

THE ANODE will become active and one or several anode spots will appear when a vacuum interrupter is used to switch a high enough ac current. The region of anode surface when an anode spot is formed is a source of particles and metal vapor emission to the switching gap even at times of several milliseconds after current zero [1]. When an appreciable recovery voltage appears across the gap, there is too much metal vapor which causes reignition and interruption failure. Presently, the formation of an anode spot is recognized as a main factor for a vacuum interrupter reaching its interrupting limit [2], [3].

The temperature of anode spot is so hot (2490 K ∼ 3040 K [4]–[6]), and it will maintain a very high temperature at current zero, even the region of the anode spot is kept in a liquid state that may be another main factor for interruption failures. Since the recovery voltage generates a strong electric field, the liquid layer can be distorted to create projections on the anode surface, which are potential sites for high-voltage breakdown and lead to an interruption failure [7]. Thus, the main phenomenon limiting the performance of a practical vacuum interrupter is closely related to the presence before current zero of the high-current anode phenomena.

Extensive research work showed that an anode phenomenon of vacuum arcs follows the arc current and contact gap [8], [9]. Miller [8]–[11] proposed a qualitative sketch of the occurrence regions for the various anode modes of a vacuum arc. In order to indicate the occurrence of an anode spot, he proposed a critical current at which an anode spot or footpoint appeared. The critical current was determined by contact gap, contact diameter, contact material, current waveform, etc. as present by Miller. Rich [12] has done considerable work to raise the critical current for the anode spot formation appreciably if the vacuum interrupter fulfills the requirements of large contact surfaces, no electrode edges, or corners, and minimizes electromagnetic forces tending to concentrate on the arc. And Kong *et al.* [13] also found that the critical current was reduced as the opening velocity increased with different contact materials.

An opening velocity characteristic was presented as a contribution factor for improving the high-current interruption performance of a vacuum interrupter [14], [15]. However, no mentioned research discussed how to improve the switching capability of a vacuum interrupter from the point of view of high-current anode phenomena. And with such an opening displacement curve, the vacuum interrupters intend to avoid the active high-current anode phenomena. The objective of this paper is to propose an opening displacement curve characteristic that is determined by high-current anode phenomena for a vacuum interrupter.

II. Experimental Setup

A test vacuum interrupter (TVI) was shown in Fig. 1. In order to observe a vacuum arc, an envelope of the vacuum interrupter is made of glass and no stainless-steel shield is used. Therefore, the anode phenomena can be observed by high-speed photography. Two different microstructures of CuCr25 (25% by weight

Manuscript received September 29, 2012; revised March 04, 2013; accepted May 07, 2013. Date of publication June 11, 2013; date of current version September 19, 2013. This work was supported in part by the National Science Foundation of China under Project No. 51177122, No. 51221005" and in part by the State Key Laboratory of Electrical Insulation and Power Equipment. Paper no. TPWRD-01029-2012.

The authors are with the State Key Laboratory of Electrical Insulation and Power Equipment, Xi'an Jiaotong University, Xi'an 710049, China (e-mail: Liuzy@mail.xjtu.edu.cn).

Color versions of one or more of the figures in this paper are available online at http://ieeexplore.ieee.org.

Digital Object Identifier 10.1109/TPWRD.2013.2264487

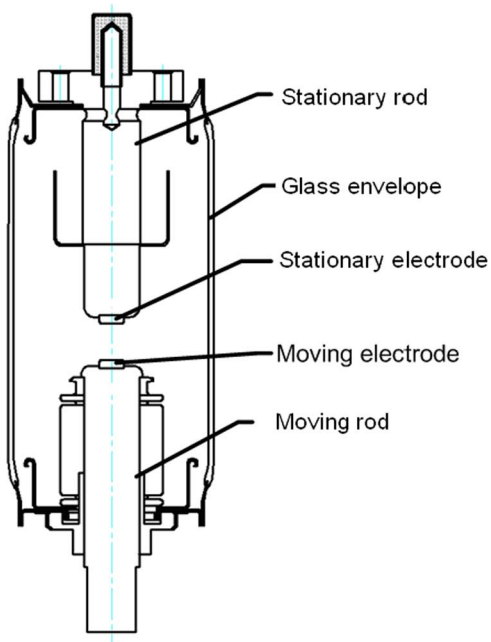

Fig. 1. Test vacuum interrupter. The envelope of the vacuum interrupter is made of glass and no stainless-steel shield is used in order to observe the anode phenomena. The diameters of the electrodes are 12 mm and 25 mm, respectively.

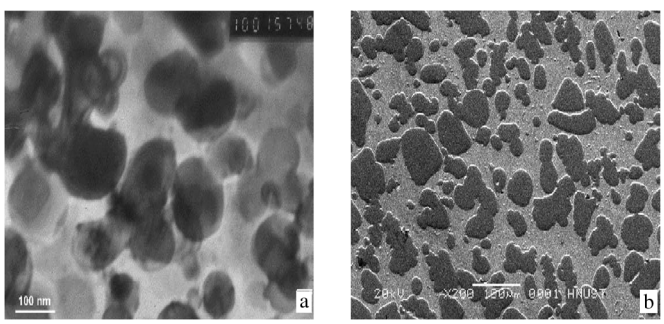

Fig. 2. Microstructures of (a) nanocrystalline and (b) microcrystalline CuCr25 alloys (25% by weight of Cr). The microstructure of nanocrystalline CuCr25 was examined by a transmission electron microscopy (TEM), scale: 100 nm per unit. And the microstructure of microcrystalline CuCr25 was examined by a scanning electron microscopy (SEM), scale: 100 μm per unit.

of Cr) contact materials were prepared as shown in Fig. 2. One is nanocrystalline CuCr25 which has a size of Cr particles less than 120 nm, as shown in Fig. 2(a). And the other one is microcrystalline CuCr25 in which the Cr particle size in Cu matrix is less than 100 μm as shown in Fig. 2(b). The processing method of contact materials and the manufacturing of the vacuum interrupter were indicated in previous work [16]. For each contact material, we prepared three vacuum interrupters of 12-mm contact diameter and three vacuum interrupters of 25-mm contact diameter, respectively.

In order to obtain an anode discharge modes diagram of each test vacuum interrupter, experiments were conducted by using an apparatus shown schematically in Fig. 3. The test vacuum interrupters were operated by a permanent-magnet operating mechanism. The electrodes of the test vacuum interrupters were controlled electronically to be separated by the mechanism, and a vacuum arc was initiated by passing a 50-Hz power

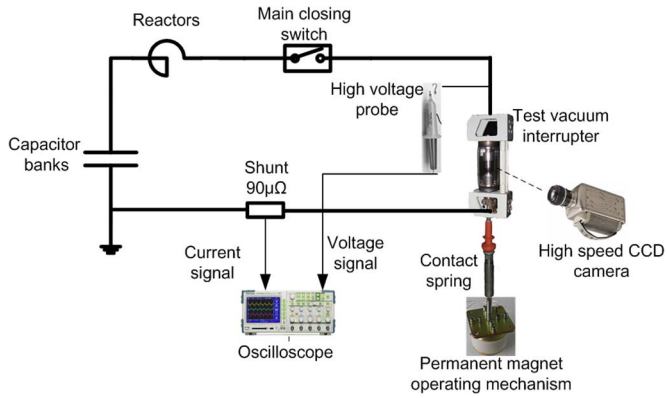

Fig. 3. Experimental circuit. A power frequency (50 Hz) current was generated by the LC discharging circuit and capacitor banks were precharged.

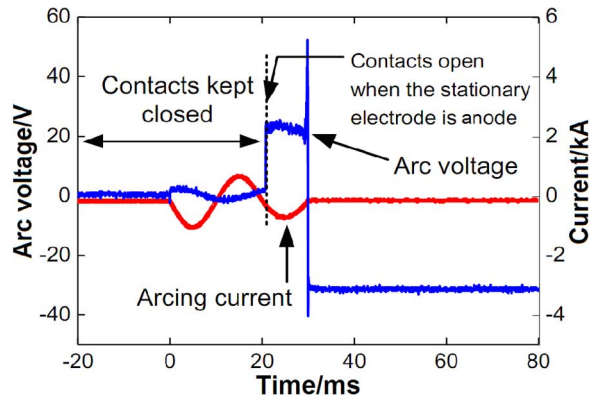

Fig. 4. Typical waveforms of arc current and arc voltage. The contacts opened at the third half-wave (the stationary electrode is an anode). The arc current is 1.5 kA (peak value). The arcing time is 9.5 ms and the arc voltage is about 20 V.

frequency current. The arcing time was adjusted in a range from ~1 ms to 10 ms. By precharging capacitor banks to an appropriate voltage, a power frequency (50 Hz) current flowed the test vacuum interrupter by passing through reactors (LC discharging circuit). The discharging current was controlled by the charging voltage of the capacitor banks. The arc voltage was measured by means of a Tektronix high-voltage probe 6015 A (1000:1) and the arc current was measured by a shunt of a 90-$\mu\Omega$ resistor, as shown in Fig. 4. And two opening velocities (1.1 m/s and 2.0 m/s) were adopted by adjusting a contact spring stroke of the mechanism from 1 to 9 mm. The opening velocity was defined as an average velocity during 10 ms after contacts separation.

We observed the vacuum arc phenomena with a high-speed charge-coupled device (CCD) video camera Phantom V10 at a speed of 10 frames/ms. Exposure time of each individual frames was 2 μs. The high-speed CCD camera kept focusing on the upper electrode (stationary electrode) which was each anode in the experiments. The contact gap between the electrodes was determined by comparing it with the size of a contact whose contact diameter was 12 or 25 mm in each frame of a camera movie. The diameter of anode spots can also be determined by this method. A frame where a first bright spot appeared was identified as the beginning of arcing and it was correlated to the instant of a voltage jump of 20 V on the arc voltage record.

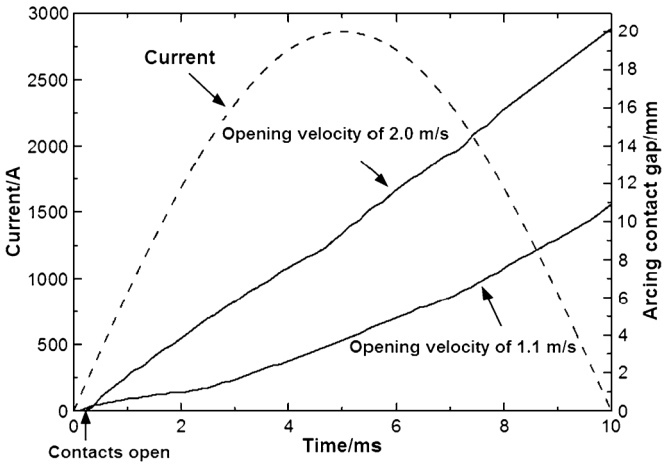

Fig. 5. Typical arc current and arcing contact gaps with an opening velocity of 2.0 and 1.1 m/s.

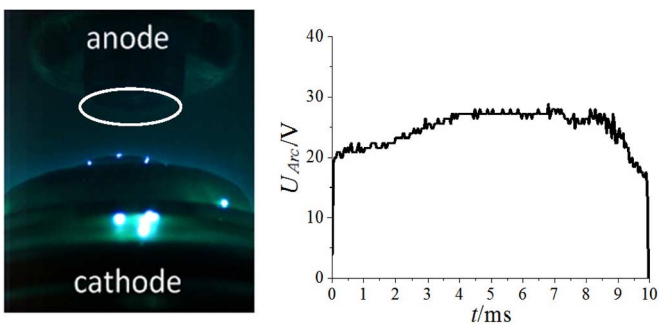

Fig. 6. Anode phenomenon and the arc voltage of a diffuse arc mode. The contact material is microcrystalline CuCr25. The contact diameter is 12 mm. The opening velocity is 2.0 m/s. The arc current is 0.5 kA (peak value). The frame is 7.5 ms before current zero.

Thus, the correlation among the anode phenomena, arcing current, arcing time, and contact gap can be obtained, as shown in Fig. 5.

III. Results

A. Anode Discharge Modes

Based on a definition of the anode phenomena proposed by Miller [2], [10], [11], we distinguished four anode discharge modes in our experiments: a diffuse arc mode, a footpoint mode, an anode spot mode, and an intense arc mode.

Diffuse arc: In the diffuse arc mode, the anode remains nonluminous. (See Fig. 6.) Throughout most of the diffuse arc mode region, the anode has only a slight effect on the overall behavior of the arc which is controlled by cathode phenomena. The arc voltage of the diffuse arc mode is quiet.

Footpoint: In contrast to the diffuse arc mode, where the anode is nonluminous, in the footpoint mode, small bright spots appear on the anode (see Fig. 7). These spots are denoted as footpoints. Footpoints are characterized as being small luminous spots, usually associated with local anode melting and with the appearance of anode material in the discharge. And the arc voltage develops significant noise components when a footpoint appears.

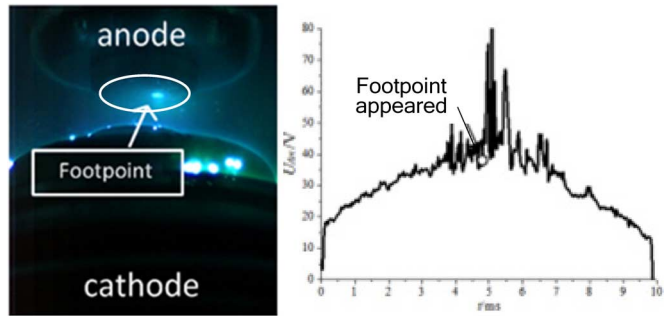

Fig. 7. Anode phenomenon and the arc voltage of a footpoint mode. The contact material is microcrystalline CuCr25. The contact diameter is 12 mm. The opening velocity is 2.0 m/s. The arc current is 1.5 kA (peak value). The frame is 5 ms before current zero in which a footpoint is formed on the anode surface.

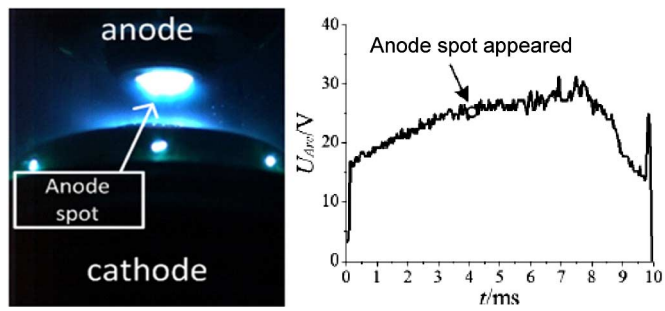

Fig. 8. Anode phenomenon and the arc voltage of an anode spot mode. The contact material is nanocrystalline CuCr25 and the contact diameter is 12 mm. The opening velocity is 2.0 m/s. The arc current is 2.5 kA (peak value) and the frame is 4.2 ms before current zero.

Anode spot: The anode spot mode is a high-current mode with a considerable anode activity. In the anode spot mode a more or less well-defined arc column appears in the interelectrode gap. One large or (less often) several small very bright spots are present on the anode (see Fig. 8). An anode spot differs from a footpoint in that it is much hotter (near the electrode material boiling point rather than its melting point), generally much larger, and evolves much greater quantities of anode material. Meanwhile, the mean arc voltage did not decrease with an anode spot formation, and the noise component decreased sharply.

Intense arc: The intense arc mode is also a high-current mode where the anode is very active. In the intense arc mode, very bright luminosity appears to cover the anode, the cathode, and fill the interelectrode gap (see Fig. 9). The intense arc mode often occurs at a lower opening velocity of 1.1 m/s with shorter gap lengths, which is very similar to the "transition diffuse arc" described by Schulman *et al.* [17]. Due to the short gap and high luminosity of the arc, the footpoint and anode spot on the anode surface cannot be distinguished in the intense arc mode. And the arc voltage is also quiet.

B. Anode Discharge Modes Diagrams

In each arcing sequence, a change of anode discharge mode that is associated with a specific arc current and contact gap value can be indicated as one point on an anode discharge diagram. The anode discharge diagram of a vacuum interrupter with microcrystalline CuCr25 contact material and 12-mm

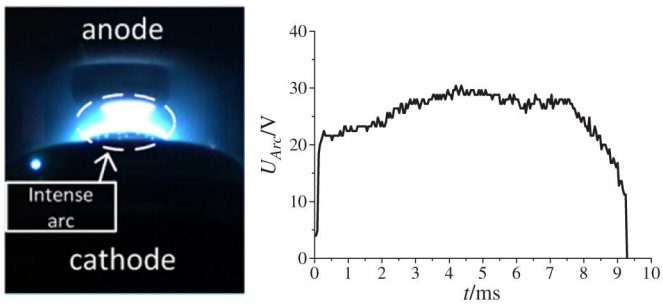

Fig. 9. Anode phenomenon and the arc voltage of an intense arc mode. The contact material is nanocrystalline CuCr25. The contact diameter is 12 mm. The opening velocity is 1.1 m/s. The arc current is 3.6 kA (peak value). The frame is 5 ms before current zero.

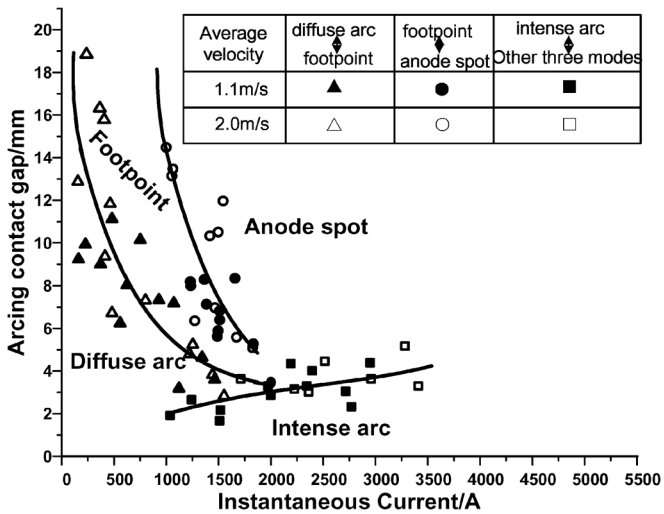

Fig. 10. Anode discharge diagram with microcrystallite CuCr25, contact diameter 12 mm. [▲], [△] data of a transfer between "diffuse arc" mode and a "footpoint" mode; [●], [○] data of a transfer between a "footpoint" mode and an "anode spot" mode; [■], [□] data of a transfer between an "intense arc" mode and the other three modes. [▲], [●], [■] data of an average opening velocity of 1.1 m/s; [△], [○], [□] data of an average opening velocity of 2.0 m/s. The critical current, which the anode discharge mode transited from footpoint to anode spot, was in the range of 1–2 kA.

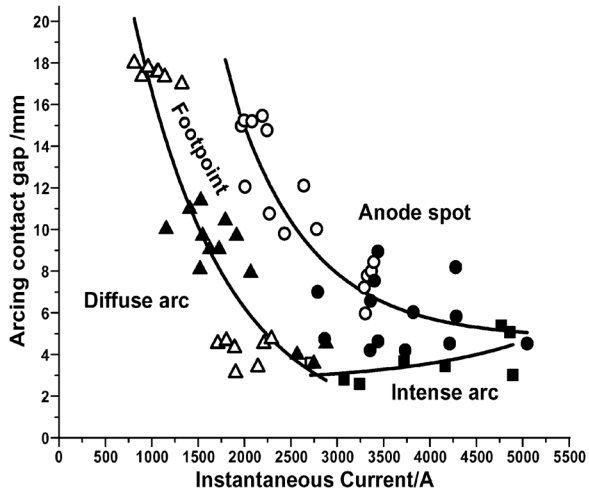

Fig. 11. Anode discharge diagram with microcrystallite CuCr25, contact diameter 25 mm. The descriptions of the symbols refer to the descriptions in Fig. 10. The critical current which the anode discharge mode transited from footpoint to anode spot was in the range of 2–5 kA.

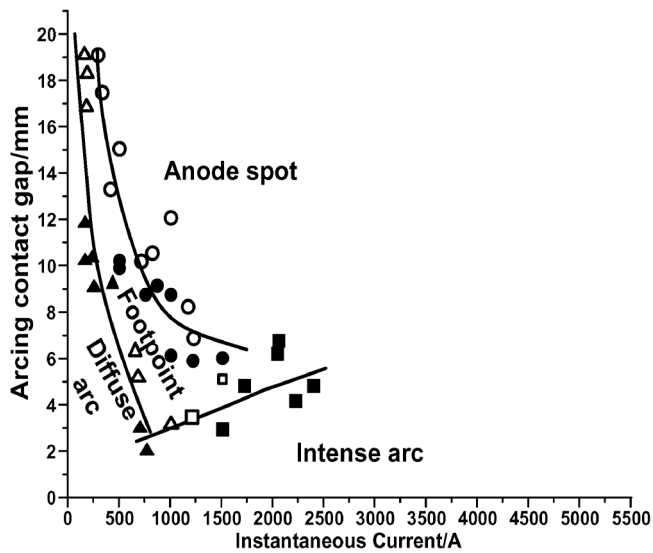

Fig. 12. Anode discharge diagram with nanocrystallite CuCr25, contact diameter 12 mm. The descriptions of the symbols refer to the descriptions in Fig. 10. The critical current which the anode discharge mode transited from footpoint to anode spot was in the range of 0.3–1.5 kA.

contact diameter was established as shown in Fig. 10. The symbol "triangle" represents a change between a "diffuse arc" and a "footpoint" anode discharge modes. Symbol "circle" represents a change between a "footpoint" and an "anode spot" anode discharge modes. And symbol "square" represents a change between an "intense arc" and the other three anode discharge modes. The solid symbols "▲, ●, ■" are in a condition that the average opening velocity was 1.1 m/s. In addition, the hollow symbols "△, □, ○" represent anode discharge modes' transition with an average opening velocity of 2.0 m/s. With a large number of transition points between anode discharge modes transition in the experiments, we can establish boundaries between regions of different anode discharge modes in an anode discharge diagram. Each type of vacuum interrupter has its own anode discharge modes' diagrams, as shown in Figs. 10–13, and the differences between these anode discharge modes' diagrams are the different boundaries of each anode discharge mode.

For different vacuum interrupters, the critical current where a footpoint or an anode spot appeared is affected by a contact diameter and contact material. Figs. 10–13 show that the anode phenomena of the nanocrystalline CuCr25 contact material took place at a lower current than that of the microcrystalline one. The experimental results also show that the critical current where the anode spot appeared will be increased with the contact diameters.

C. Relationship Between an Anode Discharge Diagram and an Opening Displacement Curve Characteristic

Based on the anode discharge mode diagrams with different contact materials and contact diameters, it was found that the opening velocity of 1.1 m/s and 2.0 m/s has no significant influence on the boundaries between each anode discharge mode.

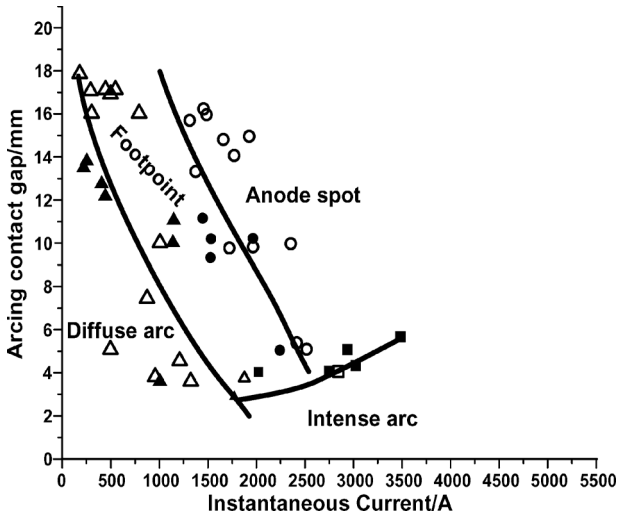

Fig. 13. Anode discharge diagram with nanocrystallite CuCr25, contact diameter 25 mm. The descriptions of the symbols refer to the descriptions in Fig. 10. The critical current which the anode discharge mode transited from footpoint to anode spot was in the range of 1.5–2.5 kA.

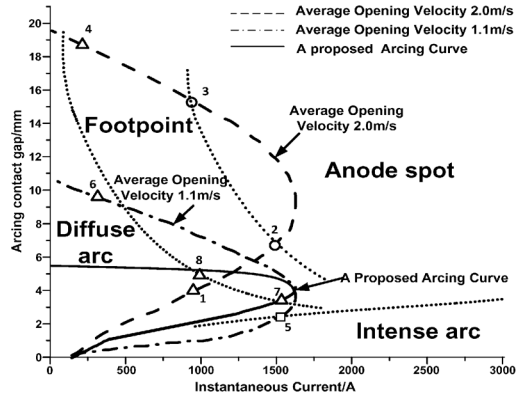

Fig. 14. Anode discharge mode diagram with three opening displacement curve characteristics. The contact material is microcrystalline CuCr25. The contact diameter is 12 mm. (- - - - - - -) is the opening curve with an opening velocity of 2.0 m/s; (— · —) is the opening curve with an opening velocity of 1.1 m/s; (———) is the proposed opening curve. The arcing curve shows the relationship between the contact gap and arc current in an anode discharge diagram. The descriptions of points 1–8 are shown in Table I. Points 1–4 show the key transition points in the arcing curve with an opening velocity of 2.0 m/s; points 5–6 show the key transition points in the arcing curve with an opening velocity of 1.1 m/s; points 7–8 show the key transition points in the proposed arcing curve.

Consequently, we expected that a specific anode discharge diagram exists for a given vacuum interrupter. And it did not change according to the opening velocity of the electrode.

Once a vacuum interrupter is used to interrupt a certain current, there is an arcing curve which is a function of arc current and arcing contact gap in an anode discharge diagram. For example, an anode discharge diagram for the vacuum interrupter with 12-mm diameter butt-type electrodes with microcrystalline CuCr25 contact material is shown in Fig. 14, and the descriptions of key transition points 1–8 are shown in Table I. We suppose that this vacuum interrupter is used to interrupt an arc current of 1650 A (peak value). Then, three different opening displacement characteristics are shown with a same arcing time of 9.5 ms. When the electrodes separate with an average velocity 2.0 m/s (as represented by a dashed line and points 1–4 were the key transition points in this curve), a diffuse arc mode formed initially. Thereafter, at a contact gap of 4.0 mm and arc current of 984 A (point 1), a footpoint formed. And even further, the vacuum arc changes into an anode spot mode when the arc current reaches 1490 A and the contact gap reaches 6.7 mm (point 2). When the arc current fell below a value of 1006 A, the anode spot converted into a footpoint mode with a contact gap of 15.0 mm (point 3). And the footpoint disappears when an arc current was lower than 214 A and a contact gap reaches 18.7 mm (point 4). Here, the vacuum arc becomes a diffuse arc.

Fig. 14 also shows that when the electrodes separate with an average opening velocity of 1.1 m/s (as represented by a dash dot line and points 5–6 were key transition points in this curve), the arcing sequence becomes better because an anode spot mode disappears. In such a case, an intense arc mode is formed first. At a gap of 2.4 mm, the intense arc transfers into a footpoint mode when an arc current reaches a value of 1528 A (point 5). And the footpoint mode disappears when the arc current falls at 315 A and the contact gap reaches 9.6 mm (point 6). After that, a diffuse vacuum arc forms.

TABLE I
DESCRIPITIONS OF POINTS 1–8 IN FIG. 14

No.	(Current, Gap)	Arc Mode	Opening Velocity
1	(984A, 4.0mm)	Diffuse arc -> Footpoint	2.0m/s
2	(1490A, 6.7mm)	Footpoint -> Anode spot	
3	(1006A, 15.0mm)	Anode spot -> Footpoint	
4	(214A, 18.7mm)	Footpoint -> Diffuse arc	
5	(1528A, 2.4mm)	Intense arc -> Footpoint	1.1m/s
6	(315A, 9.6mm)	Footpoint -> Diffuse arc	
7	(1574A, 3.3mm)	Diffuse arc -> Footpoint	Proposed arcing curve
8	(1006A, 4.9mm)	Footpoint -> Diffuse arc	

One can also design an arcing curve to avoid the regions anode spot mode and intense arc mode in the anode discharge diagram by adjusting the opening displacement curve characteristic of a vacuum interrupter. In Fig. 14, the proposed opening displacement curve characteristic was represented by a solid curve and points 7–8 were the key transition points in this curve, with which the arcing sequence becomes even better because an anode spot arc mode and an intense arc mode can be avoided. A diffuse arc mode will be formed at the beginning. Then, the arc can enter in a footpoint mode when the arc current reaches 1574 A and the contact gap reaches 3.3 mm (point 7). As the arc current increases, the peak arc current value is located in a footpoint-mode region. When the arc current falls to 1006 A and the contact gap reaches 4.9 mm (point 8), anode phenomena will disappear. The remaining vacuum arc can be a diffuse arc mode.

It is found that with an opening velocity of 2.0 m/s, the arcing curve passed through an anode spot region. While with an opening velocity of 1.1 m/s, the vacuum interrupter suffered an intense arc mode when the contact gap was low. Both an anode spot and an intense arc will overheat the anode surface of

the vacuum interrupter which has a negative impact on current interruption. Therefore, we propose the third arcing curve solid line in Fig. 14 to avoid the regions of an intense arc mode and an anode spot mode based on an anode discharge diagram. And this arcing curve is expected to have a positive impact on high-current interruption for vacuum interrupters.

From the three arcing curves shown in Fig. 14, one can convert the arcing curves into three opening displacement curves shown in Fig. 15 and the key transition points 1–8 in Fig. 14 referred to points 1′–8′ in Fig. 15. The specific descriptions of points 1′–8′ were shown in Table II. It was found that the duration of an anode spot mode was from 3.6 to 7.8 ms when an average opening velocity was 2.0 m/s, and overall the anode was active from 1.9 to 9.5 ms. When an average opening velocity was 1.1 m/s, the duration of an intense arc mode was from 0 to 3.8 ms, and an anode was active until a footpoint extinguishes at 9.3 ms. However, the proposed opening displacement curve characteristic curve will pass through a footpoint mode only, and the duration of the footpoint mode will be from 4.1 to 7.8 ms. The comparison of the high-current anode phenomena with the three opening characteristics was shown in Table III. By using the proposed opening curve, neither anode spot mode nor intense arc mode will be presented in the anode of the vacuum interrupter. And the duration when the anode is active is the shortest among the three opening characteristics, which might liberate the anode surface from a high temperature; thus, it would have a positive impact on a high-current interruption in the vacuum. A high initial velocity (2.2 m/s) at the beginning (0.9 ms) of contacts separation can keep the vacuum arc away from a region of an intense arc mode. And the opening velocity should slow down to 0.42 m/s during the arcing time from 0.9 to 10.0 ms in order to avoid the anode phenomena from an anode spot mode.

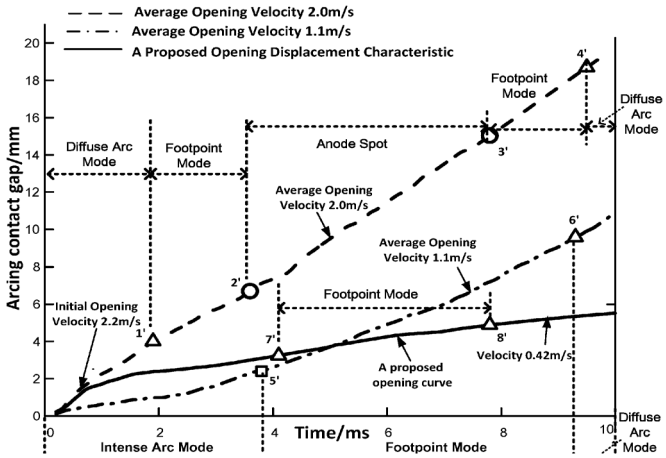

Fig. 15. Three opening displacement characteristics with different arcing curves. (- - - - - - -) is the opening curve with an opening velocity of 2.0 m/s; (— · —) is the opening curve with an opening velocity of 1.1 m/s; (——) is the proposed opening curve in which the initial opening velocity is 2.2 m/s during 0.9 ms after separate contacts, and the contact gap is 5.8 mm at current zero with a slow velocity of 0.42 m/s during the arcing time from 0.9 to 10 ms. The descriptions of points 1′–8′ are shown in Table II. Points 1′–4′ show the key transition points in the arcing curve with an opening velocity of 2.0 m/s; points 5′–6′ show the key transition points in the arcing curve with an opening velocity of 1.1 m/s; points 7′–8′ show the key transition points in the proposed arcing curve.

TABLE II
DESCRIPITIONS OF POINTS 1′–8′ IN FIG. 15

No.	(Time, Gap)	Arc Mode	Opening Velocity
1’	(1.9ms, 4.0mm)	Diffuse arc -> Footpoint	2.0m/s
2’	(3.6ms, 6.7mm)	Footpoint -> Anode spot	
3’	(7.8ms, 15.0mm)	Anode spot -> Footpoint	
4’	(9.5ms, 18.7mm)	Footpoint -> Diffuse arc	
5’	(3.8ms, 2.4mm)	Intense arc -> Footpoint	1.1m/s
6’	(9.3ms, 9.6mm)	Footpoint -> Diffuse arc	
7’	(4.1ms, 3.3mm)	Diffuse arc -> Footpoint	Proposed opening curve
8’	(7.8ms, 4.9mm)	Footpoint -> Diffuse arc	

IV. DISCUSSION

A. Effects of Contact Materials on Anode Phenomena

From the anode discharge diagram shown in Figs. 10–13, we can see that the differences between different anode discharge mode diagrams are the different boundaries of each anode mode. For different vacuum interrupters, the critical current for the anode spot formed is affected by the arc currents, the contact diameter, and the contact material. The mode diagrams of the nanocrystalline and microcrystalline CuCr25 contact materials were different. The critical current at which the anode discharge mode with microcrystalline CuCr25 12 mm contact diameter transited from footpoint to anode spot was in the range of 1–2 kA. It is higher than the critical current than with nanocrystalline CuCr25 12-mm contact diameter. Moreover, the critical current at which the anode discharge mode with microcrystalline CuCr25 25 mm contact diameter transited from footpoint to anode spot was in the range 2–5 kA. It is higher than the critical current than with the nanocrystalline CuCr25 25-mm contact diameter. Therefore, the anode phenomena of the nanocrystalline CuCr25 contact materials took place at a lower current than the microcrystalline one. One possible reason may be a lower thermal conductivity of the nanocrystalline CuCr25 contact material. Another possible reason may be that the oxygen content of the nanocrystalline contact material is higher than that of the microcrystalline contact material. The authors presented detailed information in another paper [16]. Moreover, comparing the anode discharge diagram of the same contact material with 12-mm contact diameter and 25-mm contact diameter, we can conclude that the critical current for an anode spot that was formed increased with the contact diameter. Therefore, anode phenomena appeared at very low current based on the small contacts in our experiments in comparison to other experiments [18], [19].

B. Effects of Arcing Time on the Opening Characteristic

The proposed opening curves were in a condition when an arcing time was 9.5 ms when the frequency of current is 50 Hz. However, the arcing time of an interruption in a field is uncertain due to the opening point being random when contacts separate. For example, the dashed line in Fig. 16 shows a case when the contacts separated at the current peak (1650 A, 50 Hz) with a short-arcing time of 5 ms in the anode mode diagram of

TABLE III
COMPARISON OF THE ANODE PHENOMENA WITH THE THREE OPENING CHARACTERISTICS

Opening velocity	Duration of intense arc mode	Duration of anode spot mode	Duration of active anode (including footpoint mode, anode spot mode and intense arc mode)
2.0 m/s	None	4.2 ms	7.6 ms
1.1 m/s	3.8 ms	None	9.3 ms
Proposed opening curve	None	None	3.7 ms

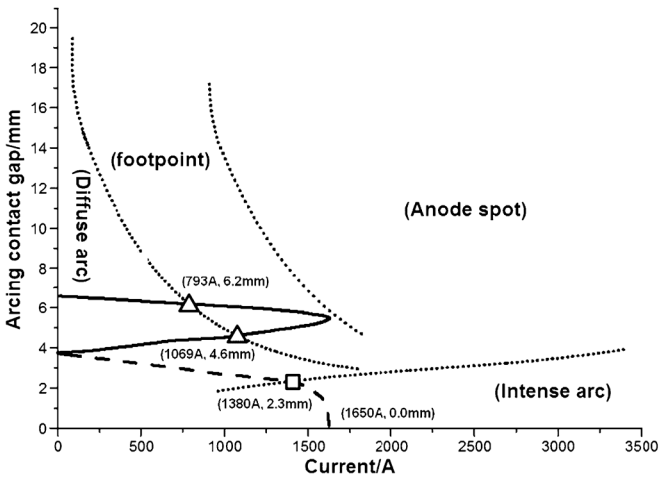

Fig. 16. Anode-mode diagram (see Fig. 10) when the contacts separate at peak current. The contact material is microcrystalline CuCr25. The diameter is 12 mm. The current is 1650 A (peak value), 50 Hz. (----) is the opening curve of an arcing time of 5 ms. And (——) is an opening curve of the second half cycle of an arcing time of 15 ms.

the vacuum interrupter with a contact diameter of 12 mm and contact materials of microcrystalline CuCr25. In such a case, an intense arc mode was formed as contacts separated. Then, the anode surface escaped fast from the intense arc mode region to the diffuse arc region when the current was 1380 A and the contact gap was 2.3 mm due to a high initial opening velocity. And the duration of intense arc is 1.8 ms as shown in Fig. 17.

Another case is with a long-arcing time (>10 ms) where the arc was reignited after the first current zero. For example, when the contacts separated at the current peak (1650 A, 50 Hz) with a long-arcing time of 15 ms, the anode phenomena of the vacuum interrupter in the first current loop (5 ms) should be the same as that in a short-arcing time of 5 ms as the dashed line shown in Fig. 16. After the first current zero, the old cathode is now the new anode in the next current loop. Assuming that the anode-mode diagram of the new anode might be expected to be the same one, a footpoint should appear on the new anode at the current of 1069 A and contact gap of 4.6 mm. Then, the anode mode should become a diffuse arc mode when the current is reduced to 793 A and the contact gap increased to 6.2 mm. Moreover, the intense arc lasted 1.8 ms on one anode at the first current loop, and a footpoint mode lasted 6.3 ms on the other anode of the second current loop as shown in Fig. 17.

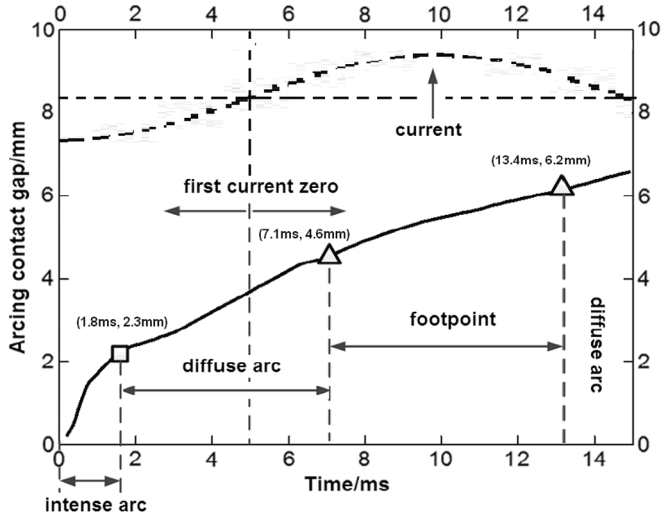

Fig. 17. Relationship between the proposed opening curve and the anode modes with an arcing time of 15 ms.

However, some interaction between anode and cathode phenomena should be a factor that influences the anode-mode diagram of the new anode in a long-arcing time. A high-current vacuum arc mode melts a local region of anode surface, such as a footpoint, an anode spot, or an intense arc. In the second half cycle of current, the old anode becomes a new cathode. The local melted region should affect a pattern of cathode spots. And the influence of the local melted cathode surface on the anode-mode diagram is not clear so far.

C. Effects of Axial Magnetic Fields on Anode Phenomena

Currently, there are two main ways of decreasing the effect of the anode spot on the interrupting performance of vacuum interrupter. The first is using a radial magnetic field to drive the arc mover over the entire contact surface. Another technique is using an axial magnetic field to inhibit the contraction of the arc column. Yanabu *et al.* [20] and Kaneda *et al.* [21] showed that the vacuum arc was controlled by a proper axial magnetic field which can increase the critical current and make uniform temperature distribution on the anode surface.

Binz and Moller [22] investigated the effect of axial magnetic field on anode modes. The arcs successively entered the diffuse arc mode, footpoint mode, and anode jet (anode spot) mode with low magnetic fields. When applying an axial magnetic field of magnitude of more than 100 mT, another anode mode called "molten anode edge" appeared on the anode surface. This was not a footpoint, but a melt spot caused by the high local energy density. Schulman *et al.* [17] also found this kind of anode mode in which the arc remained diffused in the presence of distributed anode melting. With a sufficiently strong axial magnetic field, anode melting will not occur. The reduction of plasma losses generated by an axial magnetic field can cause a vacuum arc to remain in the diffuse arc mode at currents for which it would normally have transferred to a footpoint or anode spot mode [23]–[25]. In terms of the effect of applying an axial magnetic field, the boundaries between the various modes will be shifted to higher currents. And an additional high-current anode mode ("molten anode edge") should be added on the

anode discharge mode diagrams. Therefore, further work should be done to obtain an anode-mode diagram with an axial magnetic field and propose an arcing curve which can avoid the intense arc mode, molten anode edge mode, and anode spot mode in the new diagram.

However, the investigation of anode phenomena without the axial magnetic field is still important as a start for proposing an opening displacement curve according to anode phenomena. A new design for the opening velocity should be based on the interruption capability of vacuum interrupters.

V. Conclusion

Experimental results show that opening velocities have no significant influence on mode boundaries of an anode discharge-mode diagram. Thus, an anode discharge-mode diagram can be drawn for a certain kind of vacuum interrupter according to its anode-mode observation experiments. Based on the anode discharge-mode diagram, an opening displacement curve characteristic can be proposed to prevent overheating on the anode surface by an anode spot and an intense arc mode, which is expected to have a positive impact on a high-current interruption in vacuum.

Acknowledgment

The authors would like to thank G. W. Kong and X. F. Yao, who helped finish the experiments. They would also like to thank Prof. Z. M. Yang, who provided nanocrystalline contacts and friendly discussion on contact material. This paper was presented at the 2011 1st International Conference on Electric Power Equipment—Switching Technology, Xi'an, China, October 23–27, 2011.

References

[1] J. M. Lafferty, "Triggered vacuum gaps," *Proc. Inst. Elect. Electron. Eng.*, vol. 54, no. 1, pp. 23–32, 1966.
[2] H. C. Miller, "A review of anode phenomena in vacuum arcs," *Contrib. Plasma Phys.*, vol. 29, no. 3, pp. 223–249, 1989.
[3] J. D. Cobine, "Research and development leading to the high- power vacuum interrupter—A historical review," *IEEE Trans. Power App. Syst.*, vol. PAS–80, no. 65, pp. 201–217, Apr. 1963.
[4] J. D. Cobine and E. E. Burger, "Analysis of electrode phenomena in the high-current arc," *J. Appl. Phys.*, vol. 26, no. 7, pp. 895–900, 1955.
[5] R. L. Boxman, "Measurement of anode surface-temperature during a high-current vacuum arc," *J. Appl. Phys.*, vol. 46, no. 11, pp. 4701–4704, 1975.
[6] G. R. Mitchell, "High current vacuum arcs part II—Theoretical cutline," *PIEE*, vol. 117, no. 12, pp. 2327–2332, 1970.
[7] R. E. Voshall, "Current interruption ability of vacuum switches," *IEEE Trans. Power App. Syst.*, vol. PAS-91, no. 3, p. 1219, May 1972.
[8] H. C. Miller, "Discharge modes at the anode of a vacuum-arc," *IEEE Trans. Plasma Sci.*, vol. 11, no. 3, pp. 122–127, Sep. 1983.
[9] H. C. Miller, "Vacuum arc anode phenomena," *IEEE Trans. Plasma Sci.*, vol. PS-5, no. 3, pp. 181–196, Sep. 1977.
[10] H. C. Miller, "Anode modes in vacuum arcs," *IEEE Trans. Dielectr. Elect. Insul.*, vol. 4, no. 4, pp. 382–388, Aug. 1997.
[11] H. C. Miller, "A review of anode phenomena in vacuum arcs," *IEEE Trans. Plasma Sci.*, vol. PS-13, no. 5, pp. 242–252, Oct. 1985.
[12] J. A. Rich, "A means of raising the threshold current for anode spot formation in metal-vapor arcs," *Proc. IEEE*, vol. 59, no. 4, pp. 539–545, Apr. 1971.
[13] G. W. Kong, Z. Y. Liu, D. Wang, and M. Z. Rong, "High-current vacuum arc: The relationship between anode phenomena and the average opening velocity of vacuum interrupters," *IEEE Trans. Plasma Sci.*, vol. 39, no. 6, pt. 1, pp. 1370–1378, Jun. 2011.
[14] S. Yuan, Y. Wang, and J. Wang, "Optimal moving curve of electrode to interrupt a short current for vacuum circuit breaker," in *Proc. 2nd Int. Symp. ECAAA*, Xi'an, China, 1993, pp. 248–251.
[15] J. Kusserow and R. Renz, "Method for Opening the Contact Gap of a Vacuum Interrupter," U.S. Patent 7 334 319, Feb. 26, 2008.
[16] L. Yu, J. H. Wang, Y. S. Geng, G. W. Kong, and Z. Y. Liu, "High current vacuum arc phenomena of nano-crystalline CuCr25 contact materals," *IEEE Trans. Plasma Sci.*, vol. 39, no. 6, pp. 1418–1426, Jun. 2011.
[17] M. B. Schulman, P. G. Slade, and J. V. Heberlein, "Effect of an axial magnetic field upon the developmetn of the vacuum arc between opening electric contacts," *IEEE Trans. Comp. Hyb. Manuf. Tech.*, vol. 16, no. 2, pp. 180–189, Mar. 1993.
[18] M. Bruce Schulman and P. G. Slade, "Sequential modes of drawn vacuum arcs between butt contacts for current in the 1 kA to 16 kA range," *IEEE Trans. Comp. Packag. Manuf. Technol. A*, vol. 18, no. 2, pp. 417–422, Jun. 1995.
[19] Z. Zalucki and J. Janiszewski, "Transition from constricted to diffuse vacuum arc modes during high AC current interruption," *IEEE Trans. Plasma Sci.*, vol. 27, no. 4, pp. 991–1000, Aug. 1999.
[20] S. Yanabu, S. Souma, T. Tamagawa, S. Yamashita, and T. Tsutsumi, "Vacuum arc under an axial magnetic-field and its interrupting ability," *Proc. Inst. Elect. Eng.*, vol. 126, no. 4, pp. 313–320, 1979.
[21] T. Kaneda, E. Kaneko, S. Yanabu, and H. Ikeda, "The characteristics of vacuum arcs with magnetic-fields parallel to its columns," *Phys. B & C*, vol. 104, no. 1–2, pp. 124–129, 1981.
[22] T. Binz and K. Moller, "The characteristics of high-current arcs in vacuum under the influence of axial magnetic field," *Elektrotech. Inf. Tech.*, vol. l07, pp. 134–137, 1990.
[23] E. Kaneko, T. Tamagawa, H. Okumura, and S. Yandbu, "Basic characteristics of vacuum arcs subjcctcd to a magnetic field parallel to their positive columns," *IEEE Trans. Plasma Sci.*, vol. PS-11, no. 3, pp. 169–172, Sep. 1983.
[24] J. G. Gorman, C. W. Kimblin, R. E. Voshall, R. E. Wien, and P. G. Slade, "Interaction of vacuum arcs with magnetic fields and applications," *IEEE Power App. Syst.*, vol. PAS-102, no. 2, pp. 257–266, Feb. 1983.
[25] C. W. Kimblin, "Arcing and interruption phenomena in AC vacuum switchgear and in DC switches subjected to magnetic fields," *IEEE Trans. Plasma Sci.*, vol. PS-11, no. 3, pp. 173–181, Sep. 1983.

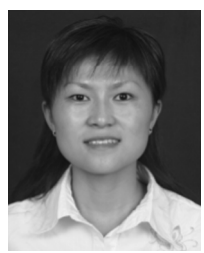

Liqiong Sun was born in Yunnan Province, China, in 1981. She received the B.S. and M.S. degrees in electrical engineering from Xi'an Jiaotong University, Xi'an, China, in 2004 and 2007, respectively, where she is currently pursuing the Ph.D. degree.

Currently, she is with the State Key Laboratory of Electrical Insulation and Power Equipment, Xi'an Jiaotong University, Xi'an, China. Her research interests focus on high vacuum interrupters, including vacuum arc, a permanent-magnet operating mechanism for high-voltage vacuum interrupters, and intelligent operations of high-voltage vacuum interrupters.

Li Yu was born in Jiangxi Province, China, in 1987. He received the B.S. and Ph.D. degrees in electrical engineering from Xi'an Jiaotong University, Xi'an, China, in 2006 and 2011, respectively.

Currently, he is with Innovation Center, Eaton, China, and Investment Co. Ltd., Shanghai, China. His research interests focus on high-voltage vacuum circuit breakers, including the contact materials, the characteristics of vacuum arcs in opening and closing operation, and the design of a high-voltage spring-type operation mechanism.

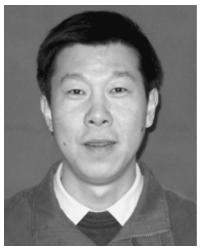

Zhiyuan Liu (M'01) was born in Shenyang, China, in 1971. He received the B.S. and M.S. degrees in electrical engineering from Shenyang University of Technology, Liaoning, China, in 1994 and 1997, respectively, and the Ph.D. degree in electrical engineering from Xi'an Jiaotong University, Xi'an, China, in 2001.

From 2001 to 2002, he was with the General Electric Company Research and Development Center, Shanghai, China. Since 2003, he has been with the State Key Laboratory of Electrical Insulation and Power Equipment, Department of Electrical Engineering, Xi'an Jiaotong University. Currently, he is a professor with Xi'an Jiaotong University. He has published more than 100 technical papers. His research interests are high-voltage vacuum circuit breakers.

Dr. Liu is a member of the Current Zero club. He is also a member of CIGRE Working Group A3.27 "The impact of the application of vacuum switchgear at transmission voltages."

Jianhua Wang received the M.S. and Ph.D. degrees in electrical engineering from Xi'an Jiaotong University (XJTU), Xi'an, China, in 1981 and 1985, respectively.

Currently, he is a Professor with the State Key Laboratory of Electrical Insulation and Power Equipment, Department of Electrical Engineering, XJTU. His research interests include theory and application of intelligent electrical apparatus systems, as well as computer-aided design/computer-aided engineering in electrical engineering.

He is the Chairman of the professional branch committee on intelligent electrical systems and its applications of the China Electrotechnical Society, the Associate Council Member of the China Electrotechnical Society, and Director of the State Key Laboratory of Electrical Insulation and Power Equipment.

Yingsan Geng (M'98) was born in Henan Province, China, in 1963. He received the B.S., M.S., and Ph.D. degrees in electrical engineering from Xi'an Jiaotong University (XJTU), Xi'an, China, in 1984, 1987, and 1997, respectively.

Currently, he is a Professor with the State Key Laboratory of Electrical Insulation and Power Equipment, Department of Electrical Engineering, XJTU. He is Director of the Department of Electrical Apparatus, XJTU. His research interests include theory and application of low-voltage circuit breakers and high-voltage vacuum circuit breakers.